

MICROMACHINING OF BRITTLE MATERIALS USING ULTRASONIC ASSISTED LAPPING

Matthew J. Klopstein, Oltmann Riemer, and Ekkard Brinksmeier
Laboratory for Precision Engineering (LFM)
University of Bremen
Bremen, Germany

INTRODUCTION

Micro-ultrasonic assisted lapping (micro-USAL) also called micro ultrasonic machining [1] or micro ultrasonic abrasive machining [2] shows promise as a manufacturing process for the small batch production of three dimensional microstructures in brittle materials. Micro-USAL was originally employed for the fabrication of holes, however with the addition of X-Y-Z stages three dimensional structures can be created. For example, Sun et al. [1] showed the use of micro-USAL and MEMS fabrication techniques in the production of a silicon air turbine with a rotor diameter of approximately $350\ \mu\text{m}$. Yu et al. [3] used micro-USAL to machine silicon with a cavity approximately $220\ \mu\text{m} \times 220\ \mu\text{m} \times 55\ \mu\text{m}$ and $1/8$ of a sphere in the center. Because brittle fracture often occurs during machining, the obtainable surface roughness is typically greater than $50\ \text{nm Sa}$ [4], [5]. This paper presents results on initial attempts to machine two dimensional structures in (100)Si with surface finish less than $50\ \text{nm Sa}$.

EXPERIMENTAL

Experiments were performed on a custom-built ultrasonic lapping apparatus which is shown schematically in Fig. 1. An ultrasonic generator mounted at the top of the frame operated at a fixed frequency of $20\ \text{kHz}$. The oscillations created by the generator were in the Z-direction and amplified by the horn to create an adjustable oscillation amplitude of $1 - 40\ \mu\text{m}$ at the tool. The tools used in this work were cylindrical tools made of tungsten carbide with a diameter of $200\ \mu\text{m}$. The workpiece was mounted to a holder which was affixed to a computer-controlled X-Y-Z stage. The stage has a positional accuracy of about $0.2\ \mu\text{m}$ in the Z-direction and about $1\ \mu\text{m}$ in the X- and Y-directions. The workpiece holder has an acoustic emission sensor mounted to it which was used to establish the location of the workpiece surface without damaging the workpiece. Two water-based slurries which contained monocrystalline diamond with an average particle size of $0.1\ \mu\text{m}$ and $0.25\ \mu\text{m}$ were used. Approximately

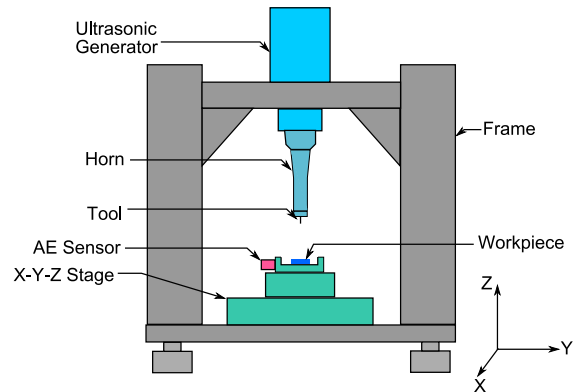


FIGURE 1. Schematic diagram of the ultrasonic lapping machine.

three to five milliliters of the slurry was placed on the workpiece prior to machining. The workpieces were cleaved from a $0.5\ \text{mm}$ thick, $100\ \text{mm}$ diameter wafer of chemo-mechanically polished (100)Si into pieces about $7\ \text{mm} \times 10\ \text{mm}$.

Two different types of structures were machined in the silicon: straight trenches and cylindrical holes. The trenches were made to investigate the achievable surface finish when machining a simple pattern. The cylindrical holes were made as simple two dimensional structures and as a preliminary step toward three dimensional structures. Before machining, the location of the workpiece relative to the tool was determined using the acoustic emission sensor. This was achieved with a computer program which moved the workpiece toward the tool in $50\ \text{nm}$ steps and after each step the acoustic emission signal was measured. The difference between the acoustic emission value at this step and the previous step was computed and compared to a threshold value. If the acoustic emission signal exceeded the threshold value, the sample was withdrawn from the tool.

Prior to a "cut" being made, the slope of the workpiece was determined by touching the tool to the surface at the beginning and end of the

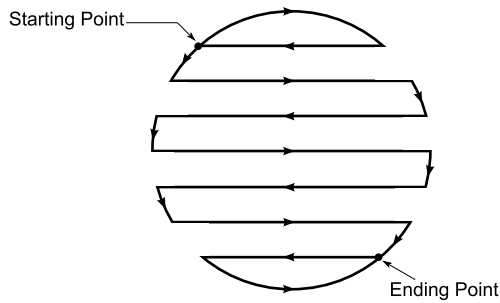


FIGURE 2. Basic tool path in the X-Y plane for cylindrical holes. The “forward” direction is shown.

cut for the straight trenches and at three points on the perimeter of a circle for the cylindrical cuts. At each of the points, the surface was touched five times and the average value was taken as the location of the workpiece surface. From the touched points, the slope was calculated in the x-direction for the trenches and in x- and y-directions for the cylindrical holes. The path of the tool was then corrected for the measured slope. For the straight trenches, the cuts were made by plunging the tool into the surface to the desired depth at the start of the cut, moving in a straight line to the end of the cut and then withdrawing the tool. The total length of a cut was 1.4 mm and the cut was in the $\langle 110 \rangle$ direction. For the cylindrical cuts a specific tool path was chosen to minimize the effects of wear on the generated surface using the uniform wear method [5]. Based on this method the desired structure was machined in layers where the basic tool path for each layer is shown in Fig. 2. The basic tool path was executed in pairs; first in the forward direction and then the tool was feed into the workpiece and the pattern was repeated in the reverse direction. For the forward direction the deepest portion of the generated cut would be at the top of the figure and tool wear would result in a shallower depth of cut at the bottom. In the reverse direction this would be reversed; the deepest portion would be at the bottom and the shallowest at the top. In this way tool wear can be taken into account. The use of this tool path to generate a cylindrical hole is described more fully below. The velocity during machining was $20 \mu\text{m/s}$ for the straight trenches and for the cylinders a velocity from $20 - 50 \mu\text{m/s}$ was used. Previous experiments with this micro-USAL equipment found that tool oscillation in the range of $1 - 6 \mu\text{m}$ had only a weak influence on the surface roughness [4] so the tool oscillation amplitude was chosen to be $3 \mu\text{m}$ for all of the

experiments presented here.

The surface roughness of the machined surfaces was measured by white light interferometry (WLI). The form and waviness of the generated surface were removed by performing a Fourier transform of the obtained image and applying an $80 \mu\text{m}$ low pass filter. For the straight trenches the area over which the roughness was obtained was $380 \mu\text{m} \times 125 \mu\text{m}$. Some of the surfaces were further examined using atomic force microscopy in the intermittent contact mode.

RESULTS AND DISCUSSION

Straight trenches were machined using $0.1 \mu\text{m}$ and $0.25 \mu\text{m}$ diamond abrasive to determine the roughness obtainable for a simple geometry. The commanded depths of cut were 3, 5, 7, and $9 \mu\text{m}$ however because of the compliance of the system the final depths were much less than the commanded values. Figure 3(a) shows the average roughness versus the final depth of cut for the case of straight trenches made with the two abrasives. The error bars denote the minimum and maximum values obtained for three cuts with two measurements at different locations for each cut. The error bars for the depth are not shown for clarity; the variation in depth was about $\pm 10\%$ of the measured depth. Figure 3(b) shows an image of part of a cut obtained by WLI with dimensions approximately $300 \mu\text{m} \times 400 \mu\text{m} \times 900 \text{nm}$ height. For cuts with a command depth greater than $3 \mu\text{m}$, the $0.25 \mu\text{m}$ diamond abrasive resulted in a higher final depth than the $0.1 \mu\text{m}$ abrasive. The roughness of the cut machined with the $0.25 \mu\text{m}$ diamond abrasive and a $9 \mu\text{m}$ command depth is not shown because it was too rough to measure with the WLI. The roughness of the cuts made with $0.1 \mu\text{m}$ abrasive was found to be less than that for the cuts made with the $0.25 \mu\text{m}$ abrasive, also the variation in roughness was less. For these reasons the $0.1 \mu\text{m}$ diamond abrasive was used for the cylindrical holes. The roughness values obtained, 5 - 15 nm, are less than values previously reported [4] in similar experiments however those values were obtained at a slightly deeper depths of cut. The only other roughness values found in the literature was for the bottom of blind holes machined in silicon and the values were from 160 - 500 nm Sa [6].

Cylindrical holes were machined in silicon with a tool path based on that shown in Fig. 2. To obtain deeper holes, the tool path was composed of

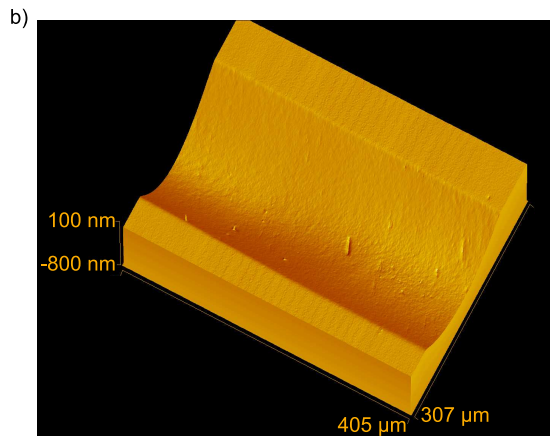
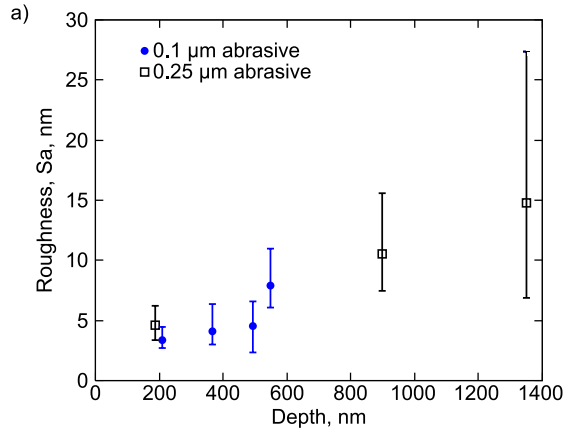


FIGURE 3. (a) Roughness versus depth of cut for 0.1 μm and 0.25 μm diamond abrasive slurries. (b) White light interferometry image of a portion of a cut made with 0.1 μm diamond abrasive.

five sets of the basic path where for each set forward and reverse directions were executed. The first set of cuts was performed as shown in Fig. 2 and the successive sets were performed with the basic pattern rotated by 72° which provided approximately 10° of overlap with the preceding cut. The command depth of cut for the five sets were the following: d , $1.5d$, $2d$, $2.5d$, $3d$, $3.5d$, $4d$, $4.5d$, $4.75d$, and $5d$ where d was the commanded depth for the first pass. The last two passes with lower depths of cut were finishing passes in an attempt to improve the surface quality.

Figure 4 shows a WLI image of a cylindrical hole approximately 1 mm in diameter with a depth of about 800 nm. This hole was made with a cutting speed of $50 \mu\text{m/s}$ however there were no significant differences observed in holes produced with a velocity of 20, 30, 40, or $50 \mu\text{m/s}$. In Fig. 4 the traces of the last cuts are clearly visible and they have a spacing of about $100 \mu\text{m}$ with a peak-

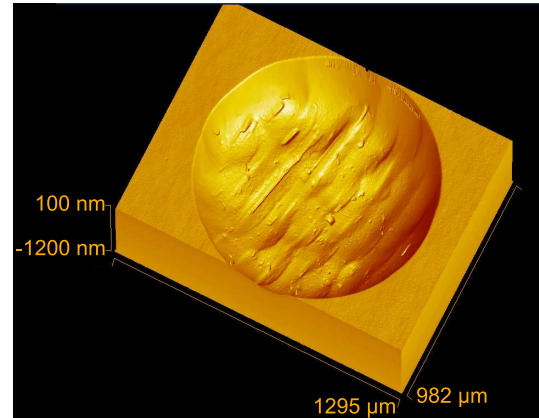


FIGURE 4. Three dimensional white light interferometry image of a 1 mm diameter cylindrical hole approximately 800 nm deep machined with a speed of $50 \mu\text{m/s}$.

to-valley of about 20 – 30 nm. The depth of the hole ranges from about 700 nm to 950 nm with the deeper portion on the right of the figure. In repeated experiments, it was found that the right portion of the hole was always lower than the left. The cause for this is not currently known but is being investigated.

Although not clearly shown in Fig. 4, the machined surfaces also contained pits which were irregularly shaped with size from $1 \mu\text{m}$ to $10 \mu\text{m}$ and a few micrometers deep. These pits typically comprised approximately 3 – 5 % of the surface area of the hole. The surface roughness in the bottom of the hole after the removal of the form and waviness was 3.4 nm Sa over a $742 \mu\text{m} \times 596 \mu\text{m}$ area. For three repeated holes made under the same conditions the roughness ranged from 3 – 17 nm Sa. In Fig. 4 it does not appear that there was severe brittle fracture of the surface however to examine the surface more closely it was measured with atomic force microscopy. Figure 5(a) shows a $1 \mu\text{m} \times 1 \mu\text{m}$ three-dimensional image and Fig. 5(b) shows a cross-section from the three-dimensional image obtained near the center of the hole. The surface is composed of peaks from 1 nm to 5 nm high and a few hundred nanometers wide. Although the sides of the peaks are not all aligned there are portions of the side surfaces that do appear aligned and could be the result of fracture. The surface roughness over the $1 \mu\text{m}^2$ area shown in Fig. 5(a) was approximately 3.7 nm Sa and over a $100 \mu\text{m}^2$ area the roughness was 4.2 nm Sa (figure not shown). Both of these values are consistent with that mea-

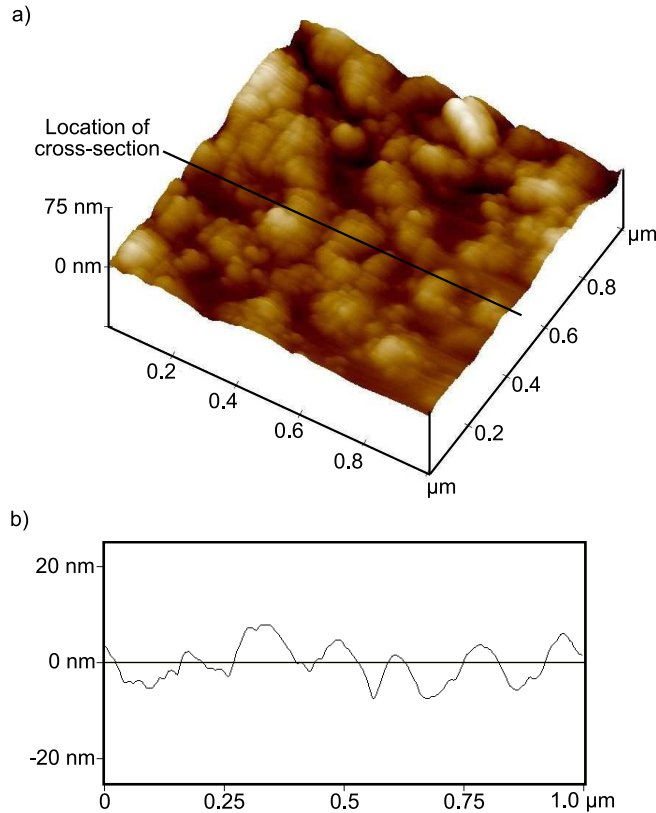


FIGURE 5. (a) AFM image of the bottom surface of hole with dimensions $1\ \mu\text{m} \times 1\ \mu\text{m} \times 150\ \text{nm}$ total height. (b) Cross-section at location shown in (a).

sured by white light interferometry.

Figure 6 shows a $400\ \mu\text{m}$ diameter hole machined with a velocity of $20\ \mu\text{m/s}$ and the same tool path as for the 1 mm diameter hole. The hole is much more rounded on the bottom with a depth in the center of about $5\ \mu\text{m}$ which is greater than the depth of the 1 mm diameter hole. Recall that the tool diameter is $200\ \mu\text{m}$ so the tool is in contact with the center of the hole for a longer time than for the 1 mm diameter hole. Note that the sidewalls of the hole are not vertical as depicted in Fig. 6; they are too steep to be accurately measured with the WLI. The surface roughness of the center portion of the hole was approximately $37\ \text{nm Sa}$ over a $240\ \mu\text{m} \times 240\ \mu\text{m}$ area. For three repeated holes, the roughness was $27 - 37\ \text{nm Sa}$ in the center portion of the hole.

SUMMARY

Initial experiments on the machining of single crystal silicon with micro-USAL were presented. The surface roughness of straight trenches was

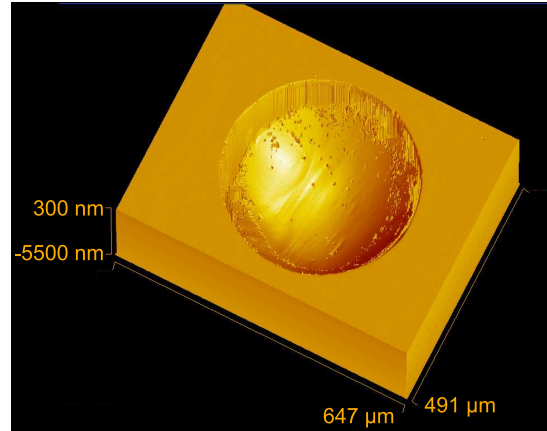


FIGURE 6. White light interferometry image of a $400\ \mu\text{m}$ diameter cylindrical hole approximately $5\ \mu\text{m}$ deep machined with a speed of $20\ \mu\text{m/s}$.

found to be in the range of $5 - 15\ \text{nm Sa}$. It was found that the $0.25\ \mu\text{m}$ diamond abrasive resulted in higher values of roughness and higher variation in roughness as compared to the $0.1\ \mu\text{m}$ diamond abrasive. The tool path for cylindrical holes was chosen consistent with the uniform wear method [5]. The surface roughness for the bottom of cylindrical holes ranged from $4 - 40\ \text{nm Sa}$. The velocity of machining in the range of $20 - 50\ \mu\text{m/s}$ was not found to have an effect on the generated surfaces.

ACKNOWLEDGMENTS

The authors gratefully acknowledge the support of the Deutsche Forschungsgemeinschaft (DFG) through grant BR825/45-1.

REFERENCES

- [1] Sun XQ, Masuzawa T, Fujino M. Micro Ultrasonic Machining and its Applications in MEMS. *Sensors and Actuators A*. 1996;57:159–164.
- [2] Kuriyagawa T, Shirozawa T, Saito O, Syoji K. Development of Micro Ultrasonic Abrasive Machining System. *JSME International Journal*. 2002;45:593–600.
- [3] Yu ZY, Rajurkar KP, Tandon A. Study of 3D Micro-Ultrasonic Machining. *Journal of Manufacturing Science and Engineering*. 2004;126:727–732.
- [4] Zhang C, Brinksmeier E, Rentsch R. Micro-USAL Technique for the Manufacture of High Quality Microstructures in Brittle Materials. *Precision Engineering*. 2006;30:362–372.

- [5] Yu ZY, Masuzawa T, Fujino M. Micro-EDM for Three-Dimensional Cavities – Development of Uniform Wear Method –. *Annals of the CIRP*. 1998;47:169–172.
- [6] Yu Z, Hu X, Rajurkar KP. Influence of Debris Accumulation on Material Removal and Surface Roughness in Micro Ultrasonic Machining of Silicon. *Annals of the CIRP*. 2006;55:201–204.